REGULAR ARTICLE

blood advances

Orally bioavailable BTK PROTAC active against wild-type and C481 mutant BTKs in human lymphoma CDX mouse models

Ye Seul Lim,[1,*] Sun-Mi Yoo,[1,*] Vineet Patil,[2,3] Han Wool Kim,[1] Hyun-Hwi Kim,[1] Beomseon Suh,[1] Ji Youn Park,[1] Na-rae Jeong,[1] Chi Hoon Park,[2,3] Je Ho Ryu,[1] Byung-Hoon Lee,[4] Pilho Kim,[2,3] and Song Hee Lee[1]

[1]Ubix Therapeutics, Seoul, Republic of Korea; [2]Therapeutics & Biotechnology Division, Korea Research Institute of Chemical Technology, Daejeon, Republic of Korea; [3]Department of Medicinal Chemistry and Pharmacology, University of Science & Technology, Daejeon, Republic of Korea; and [4]Department of New Biology, Daegu Gyeongbuk Institute of Science and Technology, Daegu, Republic of Korea

Key Points

- Although the potency of BTK degradation by UBX-382 is remarkable, cereblon neosubstrates are degraded in a cell type–dependent manner.
- UBX-382 can dramatically degrade resistance-associated mutations such as E41K, C481S/R/T/Y/F, and L528W BTKs.

Bruton tyrosine kinase (BTK) is an important signaling hub that activates the B-cell receptor (BCR) signaling cascade. BCR activation can contribute to the growth and survival of B-cell lymphoma or leukemia. The inhibition of the BCR signaling pathway is critical for blocking downstream events and treating B-cell lymphomas. Herein, we report potent and orally available proteolysis-targeting chimeras (PROTACs) that target BTK to inactivate BCR signaling. Of the PROTACs tested, UBX-382 showed superior degradation activity for wild-type (WT) and mutant BTK proteins in a single-digit nanomolar range of half-maximal degradation concentration in diffuse large B-cell lymphoma cell line. UBX-382 was effective on 7 out of 8 known BTK mutants in in vitro experiments and was highly effective in inhibiting tumor growth in murine xenograft models harboring WT or C481S mutant BTK–expressing TMD-8 cells over ibrutinib, ARQ-531, and MT-802. Remarkably, oral dosing of UBX-382 for <2 weeks led to complete tumor regression in 3 and 10 mg/kg groups in murine xenograft models. UBX-382 also provoked the cell type–dependent and selective degradation of cereblon neosubstrates in various hematological cancer cells. These results suggest that UBX-382 treatment is a promising therapeutic strategy for B-cell–related blood cancers with improved efficacy and diverse applicability.

Introduction

Bruton's tyrosine kinase (BTK) is a nonreceptor tyrosine kinase belonging to the Tec family and plays a critical role in B-cell development and adaptive immune response. B-cell receptor (BCR) activation is the first step in the signaling cascade that triggers activation of kinases, such as BTK, SYK, and phosphatidylinositol 3-kinase δ (PI3Kδ), in the plasma membrane.[1] BTK promotes the nuclear localization of NF-κB, which leads to transcriptional activation of target genes that can trigger the development, survival, and proliferation of B cells.[2] BTK functions as a significant regulator of cell proliferation and survival in B-cell malignancies.[3,4] Hence, the inhibition of BTK has emerged as one of the major strategies that can treat B-cell–related hematological cancers.

Ibrutinib, a first-in-class BTK inhibitor, has been approved by the US Food and Drug Administration and the European Medicines Agency for the treatment of B-cell malignancies including chronic lymphocytic

Submitted 18 May 2022; accepted 9 September 2022; prepublished online on *Blood Advances* First Edition 21 October 2022; final version published online 29 December 2022. https://doi.org/10.1182/bloodadvances.2022008121.

*Y.S.L. AND S.-M.Y. contributed equally to this study.

Data are available on request from corresponding authors, Song Hee Lee (shlee@ubixtrx.com) and Pilho Kim (pkim@krict.re.kr).

The full-text version of this article contains a data supplement.

leukemia (CLL)/small lymphocytic lymphoma, Waldenström macroglobulinemia, relapsed/refractory mantle cell lymphoma (MCL), and relapsed/refractory marginal zone lymphoma.[5,6] Acalabrutinib and zanubrutinib, second-generation BTK inhibitors, appear to have fewer off-target or adverse effects than ibrutinib.[7,8] However, resistance to these irreversible inhibitors has been reported mainly in patients with CLL and MCL.[9,10] Genomic sequencing analysis of patients with CLL who exhibited relapse under treatment with ibrutinib revealed mutations in the *BTK* gene.[11] Notably, the most frequent mutation was the substitution of the cysteine 481 residue with serine.[12] The C481 residue plays a critical role in the covalent binding of irreversible BTK inhibitors and the BTK protein; thus, this mutation prevents the irreversible and covalent binding of these drugs, resulting in drug resistance.[11,13] Thus, novel therapeutic options are required to overcome the drug resistance issue.

Proteolysis-targeting chimeras (PROTACs), heterobifunctional molecules that induce target protein degradation through the ubiquitin-proteasome system, have emerged as a new strategic technology in drug discovery.[14,15] PROTACs are structurally composed of 3 elements: a warhead ligand that binds to the target protein, a ligand that binds to the E3 ubiquitin ligase, and a linker that couples the 2 ligands.[16] Since its introduction in 2001,[15] PROTAC technology has innovated the concept of conventional druggability.[17] Thus far, PROTACs could expand target space by degrading various proteins such as AR, ERα, BRD2·3·4, FKBP12, BCR-ABL, and HCV NS3/4A. In addition, diverse E3 ligases such as von Hippel-Lindau, cereblon (CRBN), and inhibitors of apoptosis have been used for PROTACs.[18-23] CRBN E3 ligase binders were originally developed as immunomodulatory drugs (IMiDs) such as thalidomide, pomalidomide, lenalidomide, CC-122, and CC-885. These binders enable CRBN E3 ligase to degrade neosubstrates such as Ikaros (IKZF1), Helios (IKZF2), Aiolos (IKZF3), casein kinase 1-a (CK1-a), and G1 to S phase transition protein 1 (GSPT1).[24] CRBN binders have been widely used in designing various PROTACs owing to their ligand availability and well-characterized structure. PROTACs offer several advantages compared with traditional inhibitors. Protein degraders are characterized as event-driven mechanisms, meaning that they are competent for proteolytically targeting the protein substrate, even under transient binding.[25] Because PROTACs can use both the allosteric binding sites and the active sites of target proteins, they possess great potential to degrade undruggable proteins, such as transcription factors, nonenzyme proteins, and scaffolding proteins.[26] Furthermore, PROTACs may overcome drug resistance by eliminating overexpressed or mutated target proteins, even those with low binding affinity.[27] Therefore, PROTAC-mediated protein degradation could be a promising strategy in drug development.

Here, we report UBX-382 as a potent BTK PROTAC that exhibits extraordinary efficacy in targeting BTK and inhibiting BCR signaling in diffuse large B-cell lymphoma (DLBCL). UBX-382 showed inhibitory effects on tumor growth resulting from both wild-type (WT) and mutated BTK overexpression in in vitro and in vivo models. Moreover, UBX-382 also revealed selective degradation patterns for CRBN-IMiD neosubstrates such as Ikaros/Aiolos and GSPT1 in diverse hematological cancers, which probably reflects their diverse responses to UBX-382 treatment considering tumor growth inhibition.

Materials and methods

In vitro ternary complex formation assay

The assay was performed by combining histidine-tagged BTK (His-BTK; Thermo Fisher Scientific, PV3363), glutathione-S-transferase (GST)–tagged CRBN (Abnova, H00051185), Mab anti-6His-Eu cryptate (Cisbio, 61HISKLA), and Mab anti-GST-XL665 (Cisbio, 61GSTXLF) in a buffer (50 mM *N*-2-hydroxyethylpiperazine-*N*′-2-ethanesulfonic acid, pH 7.5, 10 mM $MgCl_2$, 1 mM EGTA, 0.01% Brij-35). Fluorescence resonance energy transfer (FRET) signals were collected at 620 nm (Eu, donor) and 665 nm (XL665, acceptor), and dose-response curves were obtained by increasing PROTAC concentrations to the donor BTK and acceptor conjugates in a final assay volume of 25 μL using a 384-well low-volume plate. The relative FRET signal was at a ratio of 665:620 and normalized against the maximum signal for the PROTAC.

Tandem ubiquitin-binding elements (TUBE1) pull-down assay

Ramos cells were seeded in a 150 mm dish and immediately treated with 0.1 μM of UBX-382 or vehicle for 2 hours at 37°C. The cells were then lysed using 50 mM Tris-HCl (pH 7.5), 150 mM NaCl, 1 mM EDTA, 1% NP-40, 10% glycerol, supplemented with Protease/Phosphatase Inhibitor (Cell Signaling Technology, 5872S) and deubiquitinase inhibitors (10 mM N-ethylmaleimide and 80 μM PR-619 [Calbiochem]) for 10 minutes. The lysates were then cleared by centrifugation. Equal amounts of supernatants were then incubated with 30 μL agarose TUBE1 beads (LifeSensors, UM401) at 4°C for 2 hours. The beads were then collected by centrifugation, washed twice by resuspending, and resuspended in a 5× sodium dodecyl sulfate buffer. The beads were then boiled for 5 minutes and analyzed by sodium dodecyl sulfate polyacrylamide gel electrophoresis. Western blotting was performed per the standard protocols.

Cell proliferation

Cells (TMD-8, OCI-LY3, U2932, TMD-8 BTK WT, TMD-8 BTK C481S, WSU-DLCL2, Su-DHL10, DOHH2, MINO, WSU-WM, K562, and MOLM13) were seeded into 96-well microplates at 500 to 2000 cells per well. Cells were treated with inhibitor or PROTAC stocks at the final concentration and incubated for 5 days, followed by a cell viability assay performed using the Cell Titer-Glo 2.0 assay kit (Promega, G9242), following the manufacturer's protocols. The plate and its contents were equilibrated at room temperature for 30 minutes before reagent addition. Cell Titer-Glo 2.0 was added at equal volumes to the cell culture media in each well. Plates were mixed for 2 minutes to induce cell lysis and incubated for 10 minutes at room temperature to stabilize the luminescent signal. The luminescent signal was measured using a microplate reader (BioTek, Synergy H1). Data were analyzed using GraphPad Prism 5.

In vivo xenograft model

CB17/severe combined immunodeficient mice were obtained from CLEA Japan, Inc and were transplanted with TMD-8 cells at 6 weeks of age. The TMD-8 cells were subcutaneously injected into the mice at a dose of 1×10^7 cells per mouse with Matrigel (Corning, 356237). Tumors reached an average volume of 180 to 200 mm^3 15 days after inoculation, after which the mice were

divided into 4 groups based on tumor size. Vehicle control or UBX-382 was then administered orally at doses of 3, 10, or 30 mg/kg once a day for 21 days. The mice were observed for 8 weeks following the final administration for tumor rebound. Tumors and body weight were measured thrice per week using calipers (Mitutoyo, CD-15APX), and tumor volume was calculated using the formula length × width^2 × 0.5. All animal experiments with mice were conducted according to guidelines approved by the Institutional Animal Care and Use Committee at Ubix Therapeutics.

Results

Characterization of the UBX-382

Of the new BTK PROTACs prepared, UBX-382 was selected based on degradation activity, metabolic stability, pharmacokinetics, and pharmacodynamics (PD). The molecule contains a novel BTK binder, a short linker, and a known thalidomide-based CRBN binder. UBX-382-Me, an N-methylated analog of UBX-382 that loses the ability to bind to CRBN, was synthesized as a negative control (Figure 1A). An in vitro TR-FRET assay was performed by varying the concentration of each PROTAC to investigate the formation of the [BTK:PROTAC:CRBN] ternary complex. The Eu-anti-His-BTK and XL665-anti-GST-CRBN pair generates a FRET signal nearby, enabling the quantitative determination of the ternary complex formation upon treatment with UBX-382 or UBX-382-Me (Figure 1B). The ternary complex formed readily as the concentration of UBX-382 increased; however, a hook effect became evident from the inflection points on the FRET curve owing to the dominance of the UBX-382:BTK and UBX-382:CRBN binary complexes at ~160 nM. As expected, UBX-382-Me did not show any FRET signals at any concentration (Figure 1B). To determine the binding affinity of UBX-382, TR-FRET–based binding assays were performed to measure the IC_{50} values of 7 compounds (UBX-382, UBX-382-Me, MT-802, ARQ-531, ibrutinib, thalidomide, and pomalidomide) in binding to BTK or CRBN. UBX-382 and UBX-382-Me showed approximately 10-fold lower binding affinities for BTK than the 2 BTK inhibitors ARQ-531[28] and ibrutinib; however, the obtained IC_{50} values were still ~2 to 3 times higher than that of MT-802, a reported BTK PROTAC (Figure 1C).[29] UBX-382 presented a binding affinity for CRBN in a micromolar range of IC_{50} that was comparable to other known CRBN ligands (thalidomide and pomalidomide) and MT-802 (Figure 1D). As expected, UBX-382-Me, ARQ-531, and ibrutinib did not bind to CRBN (Figure 1D). These results indicate that UBX-382 forms a functional ternary complex with BTK and CRBN E3 ligase to induce ubiquitination of BTK protein.

UBX-382 induces potent BTK degradation in B-cell lymphoma cell lines

To investigate the degradation activity of UBX-382, a concentration escalation assay of PROTAC was performed in the activated B-cell (ABC) DLBCL cell line TMD-8 over 24 hours. The levels of BTK protein were measured by quantitative western blotting, which yielded ~4 nM half-maximal degradation concentration of UBX-382 (Figure 2A). As expected, UBX-382-Me did not degrade BTK at any concentration. Next, time-dependent BTK degradation was examined by treating the TMD-8 cells with UBX-382 over 0.5, 1, 4, 16, 24, and 48 hours. The levels of BTK protein decreased rapidly to reach <10% after 4 hours of treatment with 100 nM UBX-382 (Figure 2B). To visualize the localization of BTK protein degraded by UBX-382, immunofluorescence was performed using confocal microscopy. The results indicated that BTK was mainly localized in the cytoplasm, as previously reported,[3] and that UBX-382 treatment significantly reduced the BTK protein levels (Figure 2C). To confirm whether the effect of UBX-382 is ubiquitin-proteasome system–dependent, a TUBE1 pull-down assay was performed to capture the ubiquitinated conjugates[30] in Ramos cells which express BTK protein. The results demonstrated that UBX-382 efficiently induced polyubiquitination and the subsequent degradation of BTK protein (Figure 2D). Moreover, we also examined the effects of the proteasome inhibitor, bortezomib, the neddylation inhibitor, MLN4924, and the autophagosome-lysosome fusion inhibitor, bafilomycin A1, under treatment with UBX-382 in cells. The amount of BTK remained unchanged when UBX-382 was cotreated with bortezomib or MLN4924 but not with bafilomycin A1, suggesting that BTK reduction occurs through ubiquitin-dependent proteasomal degradation (Figure 2E). Proteomic analysis showed that only BTK and C-terminal Src kinase were reduced as early as 4 hours after treatment with UBX-382 (Figure 2F). Overall results suggest that UBX-382 exerts highly potent and relatively selective BTK degradation through proteasomal degradation.

UBX-382 efficiently inhibits MEK and ERK signaling in B-cell lymphoma

To determine whether the PROTAC-induced BTK degradation affects downstream BCR signaling cellular activity, we examined the antiproliferative activity of UBX-382 against TMD-8, OCI-LY3, and U2932 cell lines. Consistent with a previous report,[31] ibrutinib suppressed the growth of TMD-8 cells, showing a greater inhibitory effect than that of UBX-382. Nevertheless, UBX-382 retained superior antiproliferative activity to that of ARQ-531, a reversible BTK inhibitor (Figure 3A). Because both normal and malignant B cells are known to secrete CCL3 and CCL4 in response to BCR activation,[32] we tried to confirm CCL3 and CCL4 secretion when BCR signaling was triggered by anti-IgM treatment in the TMD-8 cells. Treatment with 10 nM of UBX-382, ibrutinib, and acalabrutinib significantly abrogated CCL3 or CCL4 secretion, whereas treatment with ARQ-531, the BTK binder part of UBX-382 (Binder), and MT-802 initiated little or no effect, suggesting that inhibition of BCR signaling by UBX-382 decreases the production of chemokines CCL3 and CCL4 in TMD-8 cells (Figure 3B).

Next, we investigated whether UBX-382 could be applied to germinal center B-cell DLBCL, such as WSU-DLCL2 (Figure 3C), or ABC-DLBCL, such as OCI-LY3 and U2932 cell lines, for an antiproliferative effect (Figure 3D). UBX-382 showed greater inhibition than ibrutinib or ARQ-531 considering the proliferation of all 3 cell lines. These results indicate that UBX-382 can exert enhanced antiproliferative effects on various ABC-DLBCL cell lines. We also monitored downstream BTK signaling after BCR activation in the ibrutinib-resistant U2932 cell line. To compare the potency of the inhibitor to the degrader of BTK, an inhibitory effect on the pathway was also confirmed by measuring the direct phosphorylation activity of BTK (Y223) for all the tested compounds. Inhibition of BTK Y223 phosphorylation upon anti-IgM stimulation with UBX-382 was far more effective, compared with those of ibrutinib, acalabrutinib, and ARQ-531 in both 6- and 24-hour treated cells. (Figure 3E). In addition, UBX-382 inhibited phosphorylation of SYK, MEK, and extracellular signal-regulated

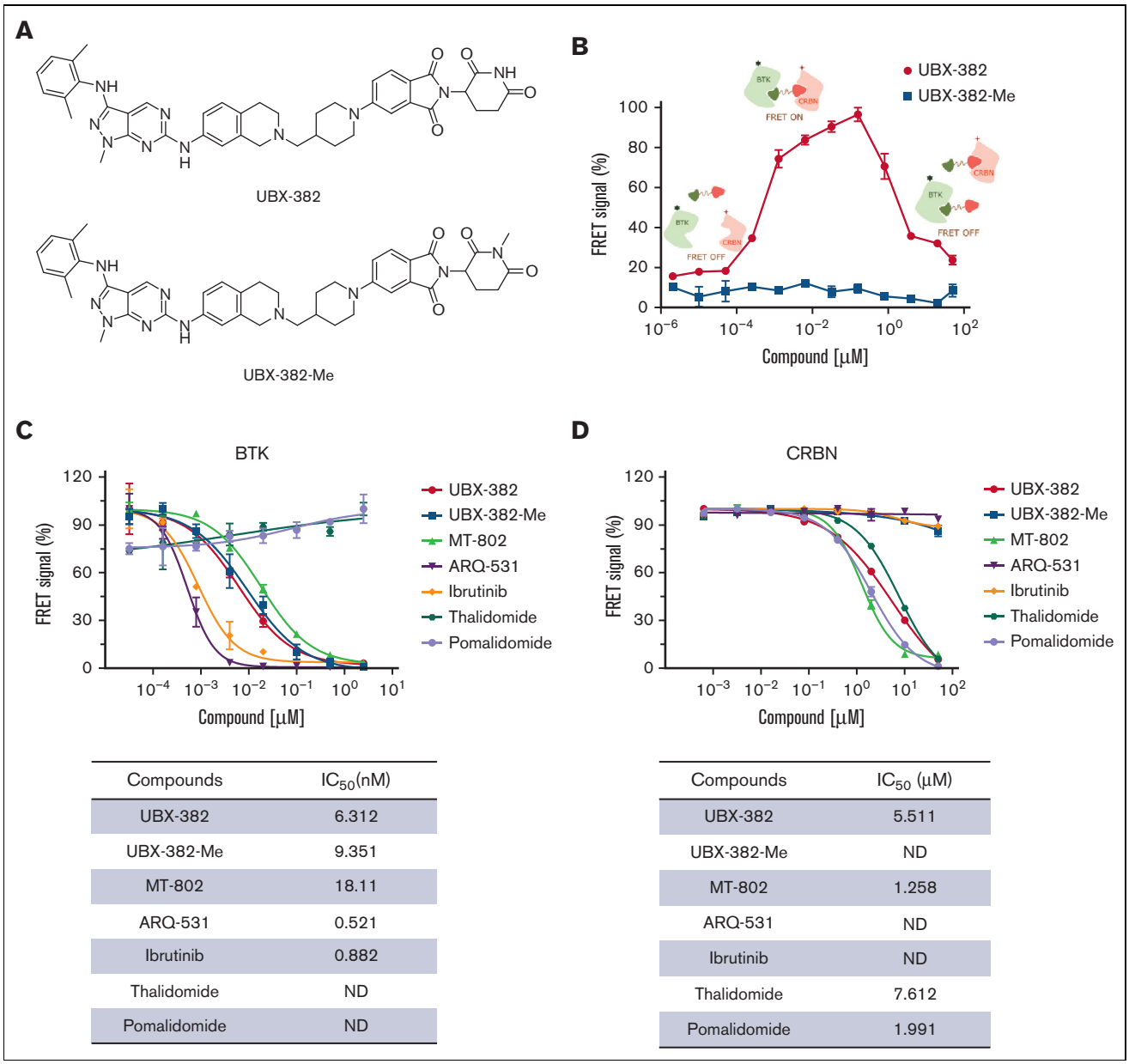

Compounds	IC_{50}(nM)
UBX-382	6.312
UBX-382-Me	9.351
MT-802	18.11
ARQ-531	0.521
Ibrutinib	0.882
Thalidomide	ND
Pomalidomide	ND

Compounds	IC_{50} (μM)
UBX-382	5.511
UBX-382-Me	ND
MT-802	1.258
ARQ-531	ND
Ibrutinib	ND
Thalidomide	7.612
Pomalidomide	1.991

Figure 1. In vitro target-binding assay. (A) Chemical structures of UBX-382 and UBX-382-Me. (B) TR-FRET–based in vitro [BTK:PROTAC:CRBN] ternary complex formation assay for UBX-382 and UBX-382-Me. Relative FRET signals represent the normalized mean of FRET signals from 2 replicates. Histidine-tagged (12 nM) and GST-tagged (20 nM) were incubated with 12 different concentrations within the range 0.002048 nM to 50 000 nM for 30 minutes and collected at 620 nm (donor) and 665 nm (acceptor). (C) BTK-target–binding assay for UBX-382 (red circle), UBX-382-Me (blue square), MT-802 (green pyramid), ARQ-531 (purple inverted pyramid), ibrutinib (yellow diamond), thalidomide (hunter green hexagon), and pomalidomide (light purple circle). 50% inhibitory concentration (IC_{50}) values of 6.31, 9.35, 18.11, 0.52, 0.88, not determined (ND), and ND were obtained for UBX-382, UBX-382-Me, MT-802, ARQ-531, ibrutinib, thalidomide, and pomalidomide, respectively. (D) CRBN-target–binding assay for UBX-382 (red circle), UBX-382-Me (blue square), MT-802 (green pyramid), ARQ-531 (purple inverted pyramid), ibrutinib (yellow green diamond), thalidomide (hunter green hexagon), and pomalidomide (light purple circle). IC_{50} values of 5.51, ND, 1.26, ND, ND, 7.61, and 1.99 were obtained for UBX-382, UBX-382-Me, MT-802, ARQ-531, ibrutinib, thalidomide, and pomalidomide, respectively. Data are represented as the mean values ± standard deviation.

kinase (ERK), partially explaining its potent antiproliferative activity in U2932 cells.

In vivo PD and UBX-382 efficacy

To evaluate PD profiles of UBX-382 as an orally bioavailable BTK degrader, UBX-382 was administered by mouth route in the mice to monitor BTK kinetics in splenic B cells using spleens collected at 3, 8, 24, and 48 hours after a single administration (Figure 4A). BTK was rapidly degraded at 3 hours, with effects lasting 24 hours after the administration of 30 mg/kg of UBX-382, before slowly increasing at 48 hours (Figure 4B). We further confirmed that PROTAC administration significantly reduced BTK levels in the

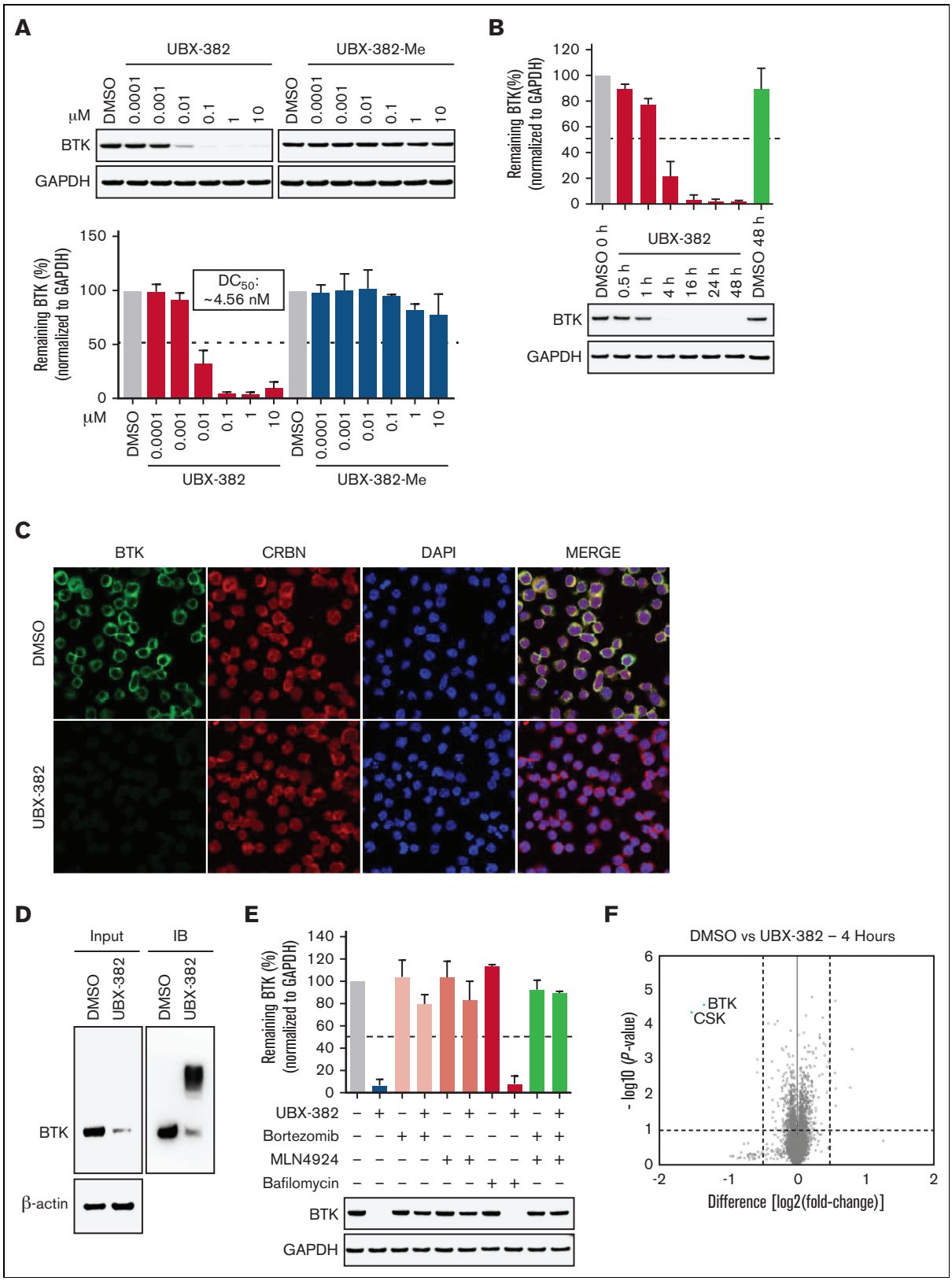

Figure 2. UBX-382 potently degrades BTK via proteasome action in B-cell malignant cell lines. (A) BTK degradation in response to increasing UBX-382 and UBX-382-Me doses in TMD-8 cells over 24 hours. BTK levels were measured by immunoblotting using specific antibodies and values for the remaining BTK were normalized using glyceraldehyde-3-phosphate dehydrogenase (GAPDH) intensity as a loading control. The results represent 2 independent experiments (n = 2). (B) Immunoblotting analysis of time-dependent degradation of BTK by treatment with UBX-382 in TMD-8 cells. The cells were treated with 100 nM UBX-382 for 0.5, 1, 4, 16, 24, and 48 hours and harvested

tumors of CB17/severe combined immunodeficient mice of the TMD-8 xenograft model (Figure 4C) by western blotting and immunohistochemistry (Figure 4D-E; supplemental Figure 1). The inhibitory effects of UBX-382 on tumor growth were investigated using TMD-8 murine xenograft models, and the data showed the daily oral administration of 10 or 30 mg/kg of UBX-382 for 3 weeks induced complete tumor regression within an average of 15 days (Figure 4F). Then 30 mg/kg of UBX-382 was administered in the 3 mg/kg dose group for a further 3 weeks, starting 7 days after the end of the initial experiment, resulting in total tumor regression. Although the tumors rebounded in 1 out of 9 mice in the 10 mg/kg group, this was not observed in the mice that were administered other doses until 84 days after the first administration (Figure 4F). No weight loss or other clinical toxicity signs were observed during the experiment (Figure 4G). These results suggest that UBX-382 shows exceptional PD efficacy and antitumor activity in mice when administered orally.

UBX-382 degrades various mutant BTK proteins in vitro and in vivo

Because resistance-associated mutations such as E41K, T474I, several C481, and L528W BTK mutants have been found in patients with CLL and patients with Richter transformation after ibrutinib treatment, UBX-382 was evaluated for the degradation activity against various BTK mutants for overcoming mutant resistance.

To investigate the degradation activity of UBX-382 against BTK mutants, diverse BTK mutants, such as E41K, T474I, C481S, C481R, C481T, C481Y, C481F, and L528W, were constructed (Figure 5A). By performing transient transfection into the HEK293 cells, each BTK protein or its phosphorylated form was monitored after treatment of UBX-382, ARQ-531, and MT-802 with 0.1, 1.0, and 10 μM of each. ARQ-531 is a reversible inhibitor that suppresses BTK activation upon BCR signaling in a C481S mutational status–independent manner.[28] MT-802 is a BTK PROTAC that can degrade C481S.[29] Here, we showed that MT-802 can also degrade E41K, C481R, C481Y, C481T, and C481F BTK mutants. Overall results suggest that UBX-382 effectively degrades WT and various BTK mutants, except for T474I, and strongly represses their phosphorylation (Figure 5B). Notably, UBX-382 appears to be far more active than ARQ-531 and MT-802 against WT and mutant BTKs.

To examine whether UBX-382 can overcome drug resistance in C481S, the antiproliferative activities of ibrutinib and UBX-382 were compared against the parent TMD-8 cells, and WT or C481S BTK–overexpressing TMD-8 cells. Overexpression of C481S BTK conferred resistance to ibrutinib treatment, which was not observed in the other TMD-8 cells. In contrast, UBX-382 significantly inhibited cell proliferation in all tested cell lines, including the C481S mutant (Figure 5C).

We then used the C481S BTK–expressing TMD-8 cells in xenograft mouse models to further evaluate UBX-382 therapeutic efficacy in the ibrutinib-resistant model. To achieve this, the tumor size in each group was measured following 3 weeks of the daily administration of 3, 10, and 30 mg/kg of UBX-382, 30 mg/kg of ibrutinib, ARQ-531, and Binder by mouth route. The results indicated that UBX-382 induced remarkable tumor regression in a dose-dependent manner, whereas ibrutinib could not inhibit tumor growth, as reported (Figure 5D; supplemental Figure 1).[33] This suggests that the antitumor activity UBX-382 can be highly enhanced in its PROTAC form, compared with that of the Binder or ARQ-531 alone. The in vivo efficacy of UBX-382 was outstanding in the TMD-8 and ibrutinib-resistant xenograft models, suggesting UBX-382 as a promising therapeutic option over BTK inhibitors for the treatment of drug-resistant hematological cancers.

UBX-382 inhibits hematological cell line proliferation via CRBN dependency

Given that UBX-382 efficiently inhibits the growth of various ABC-DLBCL cell lines in both in vitro and in vivo, its antiproliferative effect was examined using various types of hematological cell lines. We performed Cell Titer-Glo assay in germinal center B-cell–like DLBCL (Su-DHL-10), follicular lymphoma (DOHH2), MCL (Mino), chronic myeloid leukemia (K562), Waldenström macroglobulinemia (WSU-WM), and acute myeloid leukemia (MOLM13) cells with UBX-382, BTK inhibitors (ibrutinib and ARQ-531), and CRBN binders (thalidomide and lenalidomide) (Figure 6A). Compared with BTK inhibitors and CRBN binders, UBX-382 showed superior antiproliferative activity in all tested cell lines except WSU-WM, for which little effect was observed with all 5 compounds. UBX-382 greatly outperformed ibrutinib and ARQ-531 in K562, with an IC_{50} of ~2.2 nM. Two CRBN binders showed little to no effect on antiproliferation in all tested cell lines. These results suggest that UBX-382 could be a promising therapeutic agent for numerous hematological disease models, including DLBCL.

As UBX-382 diversely affects proliferation in various hematological cell lines, potential roles of CRBN were explored by treating U2932, TMD-8, DOHH-2, MINO, K562, and WSU-WM with UBX-382. Because the CRBN binder of UBX-382 is derived from

Figure 2 (continued) for the analysis of BTK levels using BTK antibody. The remaining BTK values were normalized using GAPDH intensity as a loading control. The results represent 2 independent experiments (n = 2). (C) The degradation effect of BTK by UBX-382 as determined by immunofluorescence analysis in the TMD-8 cells. Variations in BTK levels and CRBN as a result of treatment with UBX-382 for 24 hours were observed by immunofluorescence using specific antibodies as indicated in "Materials and methods." The TMD-8 cells were visualized using a confocal microscope (original magnification ×400) green, BTK; red, CRBN; and blue, nucleus. Scale bars, 20 μm. (D) BTK polyubiquitination was induced by treatment with 100 nM UBX-382 for 2 hours in Ramos cells. The polyubiquitin chains on BTK were observed using TUBE1 pull-down experiments as described in "Materials and methods." β-actin was used to confirm an equal amount of protein loading. The results represent 2 independent experiments (n = 2). (E) BTK degradation is mediated by the ubiquitin-proteasome system in TMD-8 cells. The TMD-8 cells were pretreated with 0.1 μM bortezomib, MLN4924, or bafilomycin for 1 hours and then treated with 0.1 μM UBX-382 for 4 hours. Immunoblotting was performed to verify BTK levels using specific antibodies. The immunoblotting results represent 2 independent experiments (n = 2). Data are expressed as the mean ± standard error of the mean (SEM). (F) Quantitative proteomics analysis was performed to evaluate proteome changes in TMD-8 cells. The cells were treated with 100 nM UBX-382 or dimethyl sulfoxide (DMSO) for 4 hours. Lysates were treated with the TMT-6 plex kit, which was followed by liquid chromatography-tandem mass spectrometry–based proteomics analysis. The volcano plot indicates protein ranking per the abundance ratio (log_2 fold change) for DMSO and UBX-382 and the statistical *P* value. The nonaxial vertical line represents a fold change of ± 1.5 and the nonaxial horizontal line indicates a *P* value of 0.05 significance threshold. This experiment was performed in triplicate. A total of 7418 proteins were identified in this experiment.

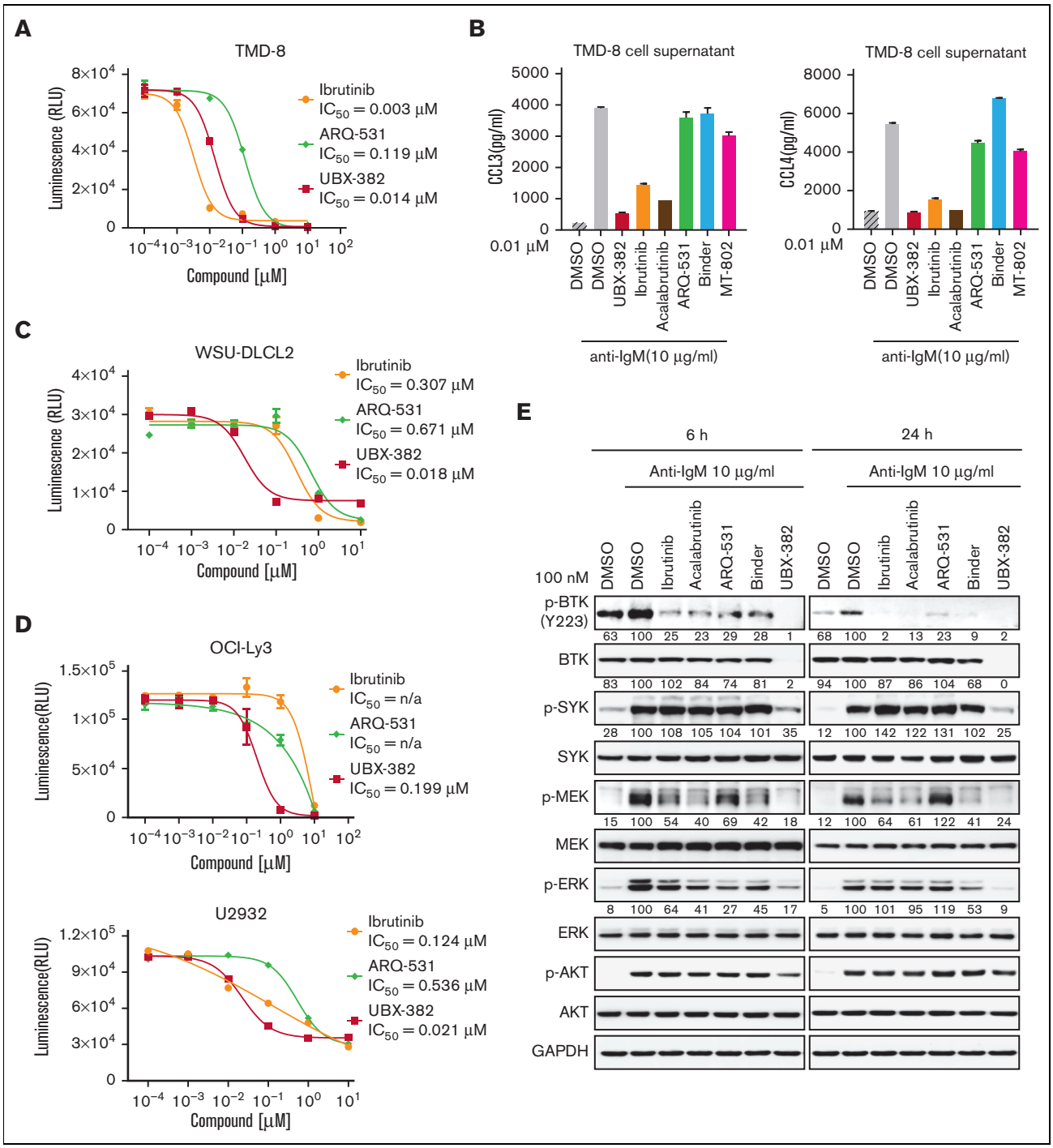

Figure 3. Inhibitory effects of UBX-382 on BCR-mediated downstream signaling. (A) Evaluation of inhibitory effects on cell proliferation by ibrutinib (yellow circle), ARQ-531 (green diamond), and UBX-382 (red square) in TMD-8 cells. The cells were seeded and treated with increasing doses of ibrutinib, ARQ-531, and UBX-382 for 3 days. Cell proliferation was measured by the Cell Titer-Glo assay in duplicates. Data are expressed as the mean ± SEM. (B) Secreted CCL3 and CCL4 levels in the TMD-8 cells. Secretion of CCL3 (left) and CCL4 (right) by the TMD-8 cells following anti–immunoglobulin M (IgM) stimulation for 8 hours and 10 nM UBX-382, ibrutinib, acalabrutinib, ARQ-531, Binder, or MT-802 for 24 hours. Each graph indicates the mean concentration of CCL3 and CCL4 produced by the TMD-8 cells cultured in a medium with DMSO, UBX-382, ibrutinib, acalabrutinib, ARQ 531, Binder, or MT-802 in the presence of 10 μg/mL anti-IgM. The experiments were performed in duplicates. Data represent the mean ± SEM. (C,D) Comparison of antiproliferative effect following treatment with ibrutinib (yellow circle), ARQ-531, and UBX-382 in WSU-DLCL2, OCI-Ly3, or U2932 cells. The cells were seeded and treated with increasing concentrations of ibrutinib, ARQ-531, and UBX-382 for 5 days. The assay was performed in duplicates. Data are expressed as the mean ± SEM. (E) Suppression of BCR-mediated signaling axis by UBX-382. U2932 cells were treated with 100 nM ibrutinib, acalabrutinib, ARQ-531, Binder, and UBX-382 for 6 and 24 hours and stimulated with 10 μg/mL anti-IgM for 15 minutes. Phosphorylation and total protein levels of BTK, SYK, MEK, and ERK were visualized via immunoblotting using indicated specific antibodies. GAPDH was used as a loading control. The quantitative results of the band intensity are labeled under the corresponding protein band (bottom). n/a, not applicable.

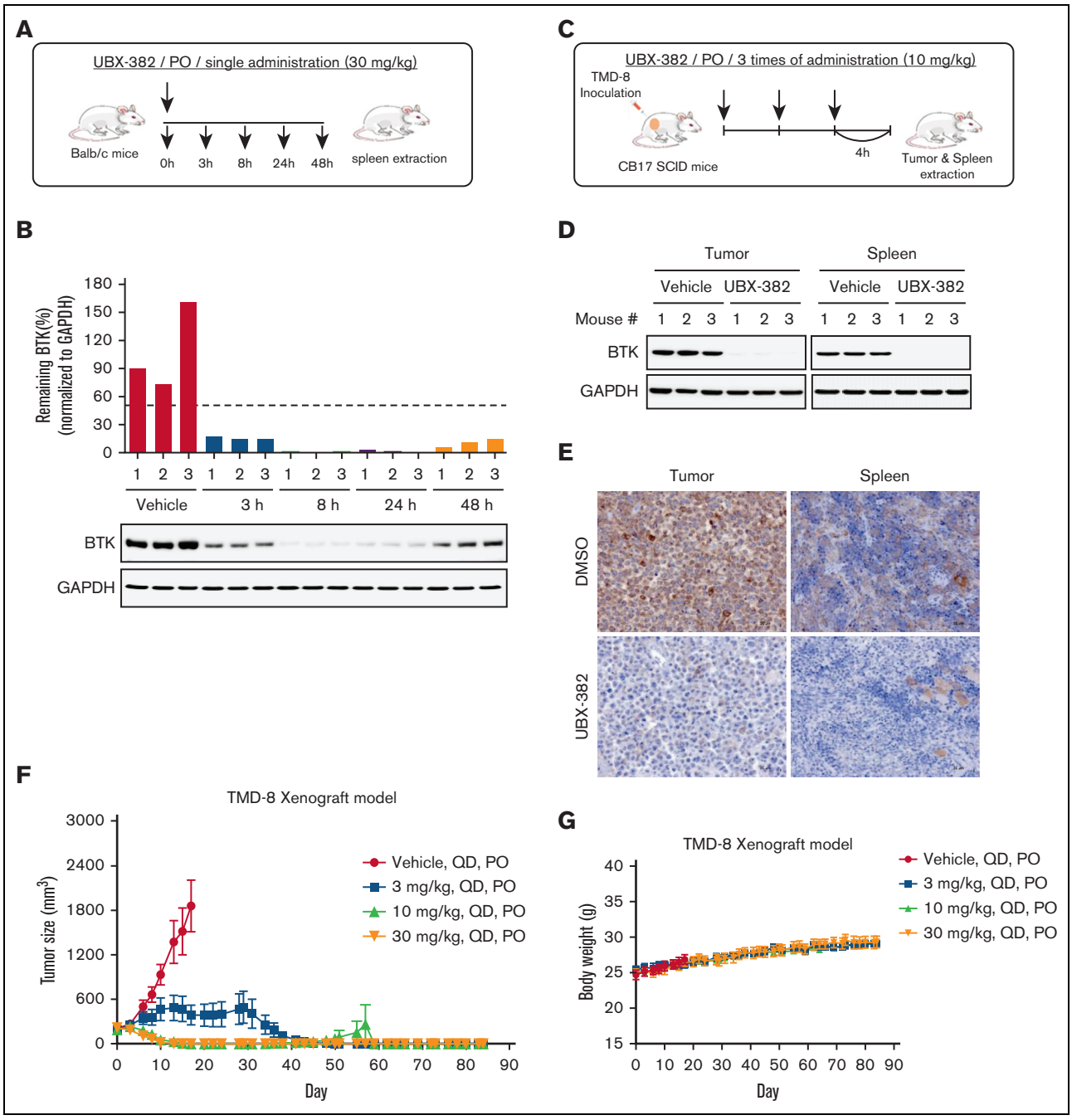

Figure 4. Evaluation of PD effect of UBX-382 in vivo. (A) Schematic overview of in vivo PD experimental design. (B) BTK levels at each dosing time (3, 8, 24, and 48 hours) were observed in spleen tissues extracted from mice (n = 3 per group). (C) Experimental scheme of in vivo PD experimental design in the xenograft model. (D) Western blot analysis of BTK levels in tumor and spleen samples of vehicle or UBX-382 treated group (n = 3 per group). (E) Immunohistochemical study of BTK levels in TMD-8 tumor and spleen tissues treated with DMSO or UBX-382. Paraffin sections of the tissues were visualized by 3,3-diaminobenzidine staining (n = 3 per group). (F) Graph showing tumor size following UBX-382 administration in the TMD-8 xenograft mouse models, with 9 mice in each group. Xenograft mice were subjected to oral UBX-382 (3, 10, and 30 mg/kg) for 3 weeks. UBX-382 was readministered to the 3 mg/kg group at a concentration of 30 mg/kg for 3 weeks 7 days after the discontinuation of the original dosing. (G) Bodyweight of CB17/severe combined immunodeficient mice treatment groups with TMD-8 xenografts after dosing with vehicle or UBX-382 (n = 9 per group). Data describing tumor growth and body weight are presented as the mean ± SEM. PO, by mouth; QD, daily.

thalidomide, we monitored the levels of Ikaros (IKZF1), Helios (IKZF2), Aiolos (IKZF3), GSPT1, and CK1-a, which are known neosubstrates of IMiD-CRBN,[34-36] upon treatment with UBX-382 or thalidomide (Figure 6B). Interestingly, BTK degradation under the treatment with UBX-382 was comparable among all the cell lines, despite different growth inhibitions. No significant change

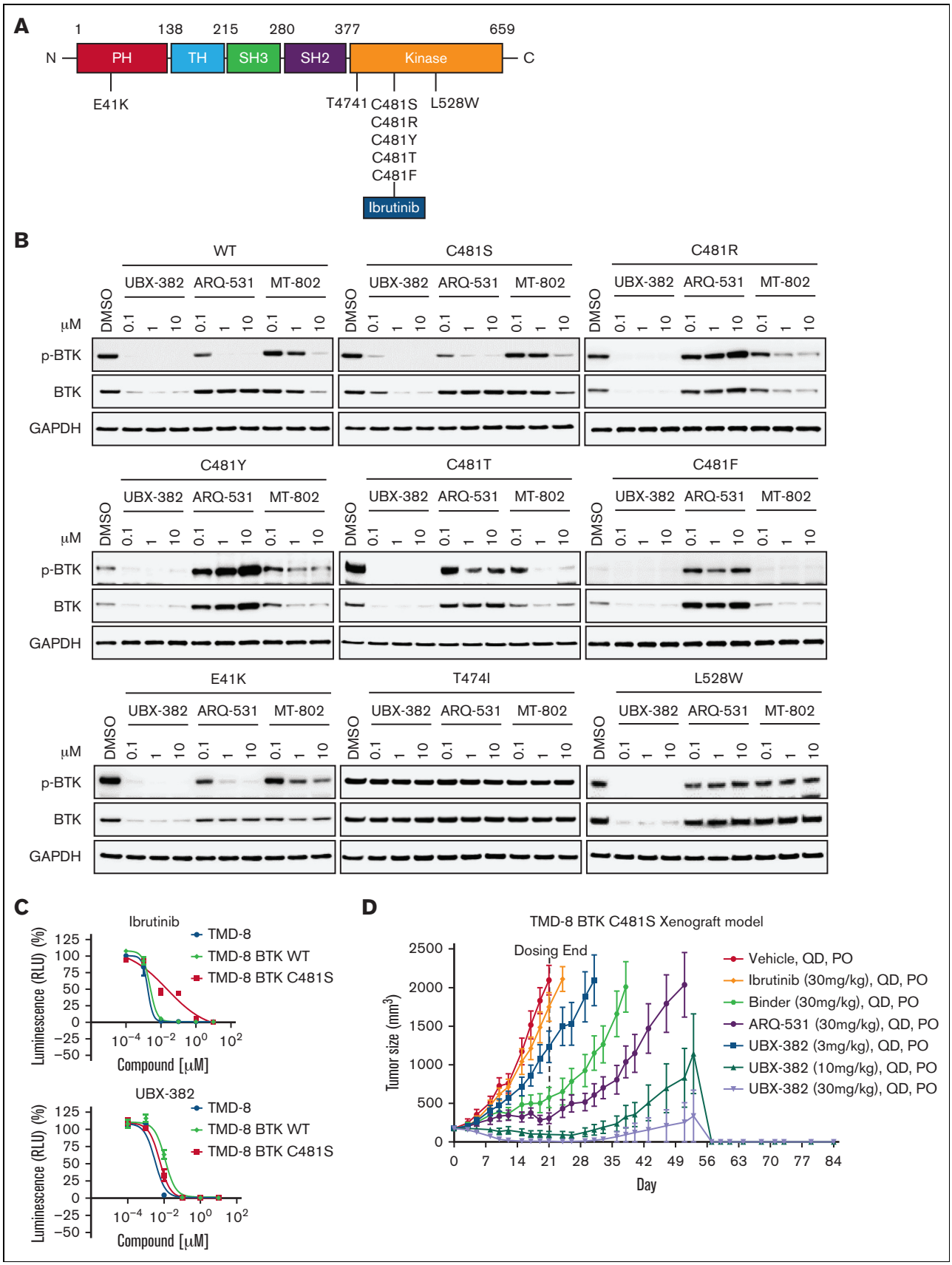

Figure 5.

was observed in the neosubstrates of U2932 and WSU-WM upon treatment with 100 nM of UBX-382 or thalidomide for 24 or 72 hours, whereas degradation of CRBN neosubstrates was highly increased in TMD-8, DOHH-2, and K562 cells after treatment with UBX-382. The protein levels of CRBN neosubstrates are given graphically for each cell line (Figure 6C). Under these conditions, thalidomide alone did not lead to any significant degradation in the CRBN neosubstrates for any of the tested cell lines. These results suggest that UBX-382 not only serves as a BTK degrader but also creates a cell type–dependent binding interface for targeting CRBN neosubstrates, which probably explains the diverse antiproliferative effects among the various hematological cell lines.

Discussion

Inhibition of BCR signaling with small molecules is a well-validated strategy for the treatment of several blood cancers.[37] A recent PROTAC approach provides an alternative solution to overcome drug-induced resistance and disease relapse that result from the action of inhibitors.[29] Although several BTK-targeting PROTACs have been described recently,[38] none of them showed in vivo efficacy against both WT and C481S mutant. We developed a potent and orally available BTK PROTAC, UBX-382, with remarkable degradation activity and excellent PD profiles for efficient cancer-targeting activity in WT and C481S mutant. The effect of UBX-382 on tumor inhibition could be further mediated through CRBN responses depending on hematological cell types.

One of the most well-known advantages of the PROTAC modality is its ability to overcome the drug resistance that results from mutation. Ibrutinib has been used successfully in several hematological and chronic graft-versus-host diseases.[39] As BTK inhibition by ibrutinib relies on its irreversible binding to the C481 site in the adenosine triphosphate–binding pocket, BTK mutations at C481 will inevitably affect patients treated with ibrutinib.[11-13] Moreover, E41K and T474I BTK mutants were also found in patients with CLL after ibrutinib treatment, and L528W is another BTK mutant found in patients with Richter transformation.[40] In particular, E41K BTK, a constitutively active and gain-of-function mutant, can promote transautophosphorylation of the BTK kinase domain and lead to overproliferation of malignant cells.[41,42] Here, we explored the inhibitory activities of UBX-382, ARQ-531, and MT-802 against 5 C481 mutants (C481S, C481R, C481Y, C481T, and C481F) and 3 other mutants (E41K, T474I, and L528W) of BTK. ARQ-531 is an adenosine triphosphate–competitive and reversible inhibitor that does not interact with C481, theoretically suggesting that C481 mutants do not interfere with its inhibitory activity. As previously reported,[28] BTK phosphorylation was substantially attenuated in ARQ-531–treated C481S and E41K BTK mutants (Figure 5B). However, the other 6 BTK mutants were only slightly affected by ARQ-531 when in phosphorylated form. By contrast, MT-802 and UBX-382 PROTACs were competent in phosphorylation degradation and suppression in the WT and most BTK mutants, highlighting an advantage of PROTACs overactive site–directed inhibitors. Notably, UBX-382 outperformed MT-802 in WT and all sensitive BTK mutants, whereas L528W was sensitive only to the treatment of UBX-382. The T474I mutant was resistant to all 3 BTK-targeting compounds used.[43] The in vitro potency of UBX-382 in the degradation of BTK mutant was also reflected in the in vivo tumor growth inhibition of a murine xenograft model using C481S-expressing TMD-8 cells (Figure 5D). Therefore, UBX-382 could provide an alternative solution for patients of hematological cancers with diverse BTK mutants acquired from the treatment of first-line or second-line BTK inhibitors.

Another merit of the PROTAC modality is the maximization of target inhibition by event-driven proteolysis, compared with conventional inhibitors.[44,45] Although the molecular weight of UBX-382 is ~2 times higher than that of the Binder, UBX-382 showed more prominent antitumor activity than the Binder and other BTK inhibitors upon the administration of the same dose (30 mg/kg) in the in vivo mouse models (Figure 5D). A similar phenomenon was reported for ARV-771 PROTAC and JQ1 binders.[46] Therefore, our data showed that efficacies from PROTAC-induced degradation could exceed activities from the Binder, which may be strongly advantageous considering dose reduction in clinical conditions.

In particular, although complete degradation of BTK was observed both in vitro and in vivo as a result of UBX-382 treatment, degradation patterns of CRBN neosubstrates were variable in a cell type–dependent manner in all cell lines used, to some extent complying with a recent report on tissue-specific differences of the BTK-degrader effect.[47] We speculate that this cell type–dependent CRBN effect may occur under different environments of ubiquitination systems. The diverse expression level of the POI and CRBN may affect the ratio of productive PROTAC-containing ternary complexes to neosubstrate-targeting IMiD-CRBN complexes. This stoichiometric alteration might also be determined by neddylation of the Cullin complex, deubiquitinating activities, or other unknown host factors. Hematological cell lines may respond differently to signaling pathways such as NF-κB, BCR-ABL, Janus kinase–signal transducer and activator of transcription, PI3K/Akt/mTOR, and/or MAPK,[48,49] which might differentially reprogram cellular networks such as the ubiquitin-proteasome machinery.

Overall, UBX-382 is potent in inducing BTK degradation, which can be applied in various hematological in vitro disease models. UBX-382 also exhibited outstanding degradation potency against various mutant BTKs, expanding its application feasibility to patients with recurrent cancers who have received prior treatment with BTK inhibitors. Furthermore, oral administration of UBX-382

Figure 5. Potent degradation and inhibition of mutated BTK in vitro and in vivo with UBX-382 treatment. (A) Schematic domain structure of BTK with known mutant sites (B) Transient-expressing WT or various mutant BTK in HEK293 cells were treated with UBX-382, ARQ-531, or MT-802 for 24 hours in a concentration-dependent manner (0.1, 1, and 10 μM). BTK levels and Y223 phosphorylation were visualized by immunoblotting. GAPDH was used as an internal loading control. Data were obtained from 2 independent experiments (n = 2). (C) Parental TMD-8 cells, WT-, or C481S BTK–overexpressed TMD-8 cells were treated with the indicated concentration of ibrutinib or UBX-382 for 5 days to measure the inhibitory effect on proliferation. These experiments were performed in duplicates by Cell Titer-Glo 2.0 Assay. Data are presented as the mean ± SEM. (D) UBX-382 showed antitumor effects in TMD-8 BTK C481S in vivo models and induced tumor remission. TMD-8 BTK C481S cells were inoculated subcutaneously into the right flank of male CB17/severe combined immunodeficient mice. When tumors had reached over 180 to 200 mm^3, the mice were divided into 7 groups and subjected to oral treatment with a control vehicle (n = 7), ibrutinib (30 mg/kg, n = 7), Binder (30 mg/kg, n = 7), ARQ-531 (30 mg/kg, n = 7), and UBX-382 (3, 10, 30 mg/kg, n = 7), respectively, each day for 21 days. Tumor volume (mean ± SEM) was observed for 84 days.

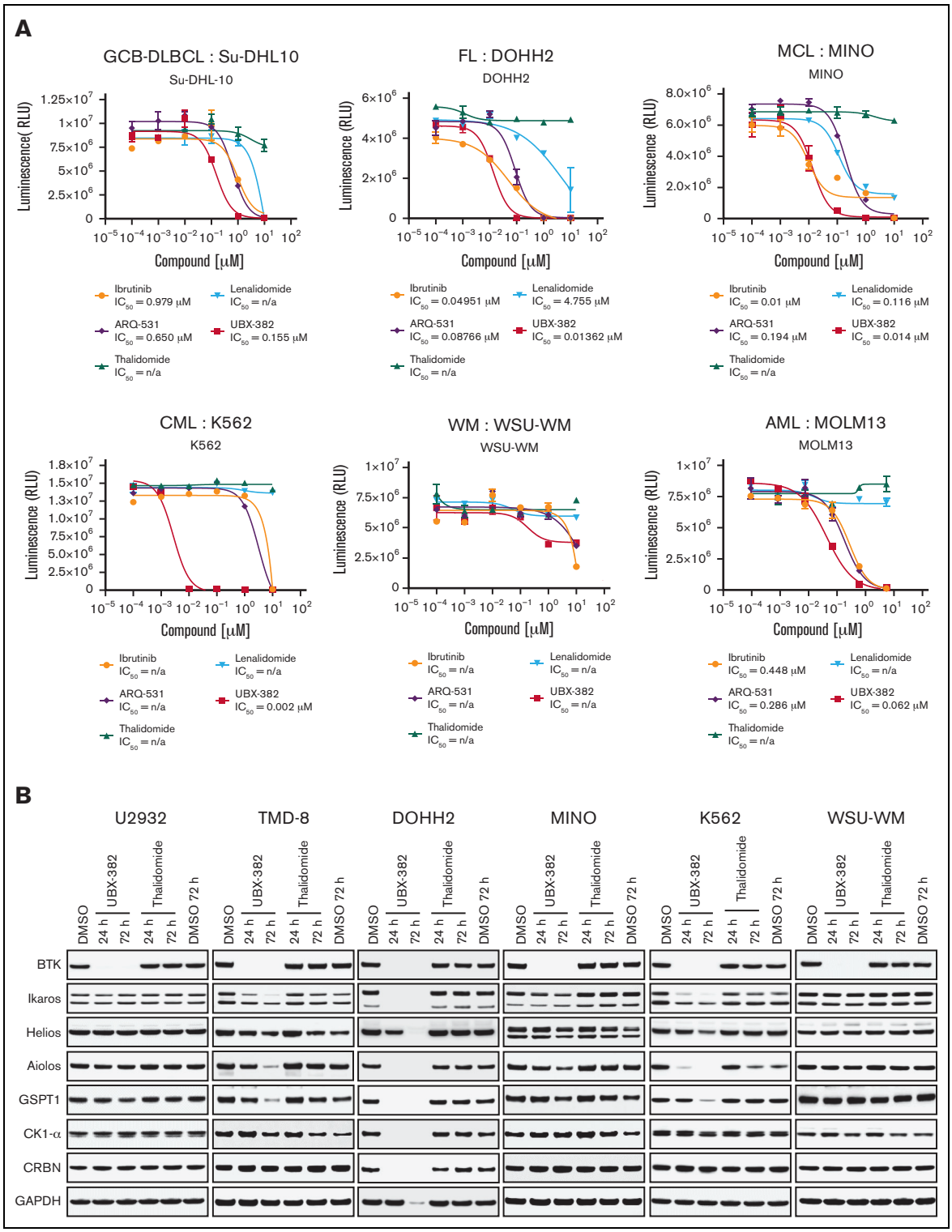

Figure 6. Validation of the antiproliferative activity of UBX-382 in diverse cell lines derived from hematological malignancies. (A) Inhibitory effects of ibrutinib (yellow circle), ARQ-531 (purple diamond), Thalidomide (hunter green triangle), Lenalidomide (sky blue inverted triangle), and UBX-382 (red square) on cell proliferation in the examined cell lines at the indicated increasing doses were monitored for 5 days by performing Cell Titer-Glo 2.0 Assay. Germinal center B-cell (GCB)–like DLBCL cell line: Su-DHL10; multiple myeloma cell line: U266; follicular lymphoma (FL) cell line: DOHH2; MCL cell line: MINO; chronic myeloid leukemia (CML) cell line: K562; and acute myeloid leukemia (AML) cell line: MOLM13. Experiments were performed in duplicates. All data are expressed as the mean ± SEM. (B) Immunoblotting analysis of BTK degradation and CRBN neosubstrates after treatment with UBX-382 and thalidomide. Hematological cell lines (U2932, TMD-8, DOHH2, MINO, K562, and WSU-WM) were treated with 100 nM thalidomide and UBX-382 for 24 hours and 72 hours. Immunoblotting was performed to verify the levels of BTK, Ikaros, Helios, Aiolos, GSPT1, and CK1-α using specific

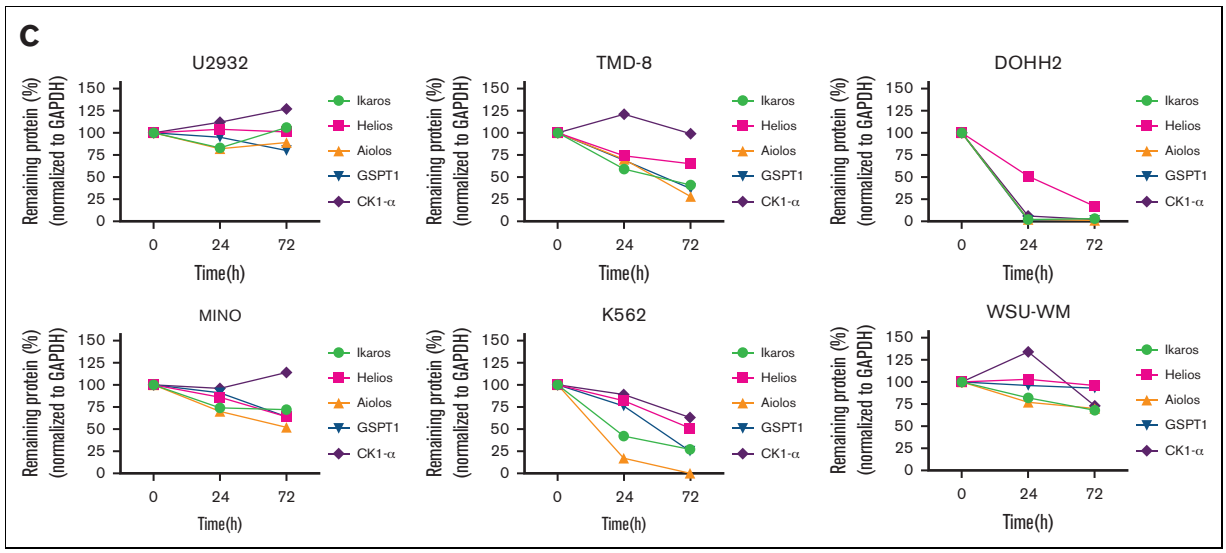

Figure 6 (continued) antibodies. (C) CRBN neosubstrate protein levels were measured by immunoblotting and values of the remaining substrates, Ikaros, Aiolos, GSPT1, and CK1-α, were normalized using GAPDH intensity value as a loading control. WM, Waldenström macroglobulinemia.

exhibited excellent in vivo efficacy in murine xenograft models using BTK WT- and mutant-expressing ABC-DLBCL cells. Because UBX-382 degrades BTK as well as diverse CRBN neosubstrates depending on cell lines, it could be applicable for the tailored treatment of B-cell malignancies. The compelling results of UBX-382 as a highly potent and efficient degrader suggest that UBX-382 could be a promising preclinical candidate for various hematological malignancies.

Acknowledgments

The authors thank all employees of Ubix Therapeutics, Inc.

This work was supported in part by a grant from the Korea Health Technology R&D Project through the Korea Health Industry Development Institute (KHIDI), funded by the Ministry of Health & Welfare, Republic of Korea (grant HI20C1021), the Korea Research Institute of Chemical Technology (grants KK1931-10 and IIT20-11), the National Research Foundation of Korea (NRF) grant, and the DGIST program of the Ministry of Science and ICT of Korea (grants 2022R1A4A2000703 and 22-CoE-BT-04) (B.-H.L.).

Authorship

Contribution: H.-H.K. measured cereblon or Bruton tyrosine kinase–binding activity; Y.S.L., S.-M.Y., H.W.K., B.S., J.Y.P., and N.-r.J. performed and designed experiments, analyzed data, assembled, and wrote the manuscript together with S.H.L.; S.-M.Y., B.-H.L., and J.H.R. revised and wrote the manuscript; C.H.P. established stable cell lines; V.P. and P.K. designed and synthesized the proteolysis-targeting chimeras; and S.H.L. supervised the experiments.

Conflict-of-interest disclosure: S.H.L. and J.H.R. are shareholders in Ubix Therapeutics and have ownership interests (including stock, patents, etc). Patent 10-2021-0083326 is held on UBX-382. A patent application on this work has been filed by Ubix Therapeutics, Inc on behalf of the authors. B.-H.L. is shareholder in Ubix Therapeutics. Y.S.L., S.-M.Y., H.W.K., H.-H.K., B.S., J.Y.P., and N.-r.J. are employees of Ubix Therapeutics and have ownership interests (including stock, patents, etc) in Ubix Therapeutics. P.K. is one of the inventors of the patent. The remaining authors declare no competing financial interests.

ORCID profiles: Y.S.L., 0000-0003-4975-6864; V.P., 0000-0003-1307-1425; S.H.L., 0000-0001-9471-5151.

Correspondence: Song Hee Lee, Ubix Therapeutics, #1508, 7, Beobwon-ro 11-gil, Songpa-gu, Seoul 05836, Republic of Korea; email: shlee@ubixtrx.com; and Pilho Kim, Therapeutics & Biotechnology Division, Korea Research Institute of Chemical Technology, 141 Gajeong-ro, Yuseong-gu, Daejeon, 34114 Republic of Korea; email: pkim@krict.re.kr.

References

1. Burger JA, Wiestner A. Targeting B cell receptor signalling in cancer: preclinical and clinical advances. *Nat Rev Cancer*. 2018;18(3):148-167.
2. Shinners NP, Carlesso G, Castro I, et al. Bruton's tyrosine kinase mediates NF-kappa B activation and B cell survival by B cell-activating factor receptor of the TNF-R family. *J Immunol*. 2007;179(6):3872-3880.
3. Hendriks RW, Yuvaraj S, Kil LP. Targeting Bruton's tyrosine kinase in B cell malignancies. *Nat Rev Cancer*. 2014;14(4):219-232.

4. Pal Singh S, Dammeijer F, Hendriks RW. Role of Bruton's tyrosine kinase in B cells and malignancies. *Mol Cancer*. 2018;17(1):57.
5. Aw A, Brown JR. Current status of Bruton's tyrosine kinase inhibitor development and use in B-cell malignancies. *Drugs Aging*. 2017;34(7):509-527.
6. Wen T, Wang J, Shi Y, Qian H, Liu P. Inhibitors targeting Bruton's tyrosine kinase in cancers: drug development advances. *Leukemia*. 2021;35(2):312-332.
7. Wu J, Zhang M, Liu D. Acalabrutinib (ACP-196): a selective second-generation BTK inhibitor. *J Hematol Oncol*. 2016;9:21.
8. Tam CS, LeBlond V, Novotny W, et al. A head-to-head phase III study comparing zanubrutinib versus ibrutinib in patients with Waldenström macroglobulinemia. *Future Oncol*. 2018;14(22):2229-2237.
9. Sedlarikova L, Petrackova A, Papajik T, Turcsanyi P, Kriegova E. Resistance-associated mutations in chronic lymphocytic leukemia patients treated with novel agents. *Front Oncol*. 2020;10:894.
10. Lewis KL, Cheah CY. Non-covalent BTK inhibitors-the new BTKids on the block for B-cell malignancies. *J Pers Med*. 2021;11(8).
11. Woyach JA, Furman RR, Liu TM, et al. Resistance mechanisms for the Bruton's tyrosine kinase inhibitor ibrutinib. *N Engl J Med*. 2014;370(24):2286-2294.
12. Woyach JA, Ruppert AS, Guinn D, et al. BTK(C481S)-mediated resistance to ibrutinib in chronic lymphocytic leukemia. *J Clin Oncol*. 2017;35(13):1437-1443.
13. Xu L, Tsakmaklis N, Yang G, et al. Acquired mutations associated with ibrutinib resistance in Waldenström macroglobulinemia. *Blood*. 2017;129(18):2519-2525.
14. Collins I, Wang H, Caldwell JJ, Chopra R. Chemical approaches to targeted protein degradation through modulation of the ubiquitin-proteasome pathway. *Biochem J*. 2017;474(7):1127-1147.
15. Sakamoto KM, Kim KB, Kumagai A, Mercurio F, Crews CM, Deshaies RJ. Protacs: chimeric molecules that target proteins to the Skp1-Cullin-F box complex for ubiquitination and degradation. *Proc Natl Acad Sci U S A*. 2001;98(15):8554-8559.
16. Gadd MS, Testa A, Lucas X, et al. Structural basis of PROTAC cooperative recognition for selective protein degradation. *Nat Chem Biol*. 2017;13(5):514-521.
17. Qi SM, Dong J, Xu ZY, Cheng XD, Zhang WD, Qin JJ. PROTAC: an effective targeted protein degradation strategy for cancer therapy. *Front Pharmacol*. 2021;12:692574.
18. Frost J, Galdeano C, Soares P, et al. Potent and selective chemical probe of hypoxic signalling downstream of HIF-α hydroxylation via VHL inhibition. *Nat Commun*. 2016;7:13312.
19. Fischer ES, Böhm K, Lydeard JR, et al. Structure of the DDB1-CRBN E3 ubiquitin ligase in complex with thalidomide. *Nature*. 2014;512(7512):49-53.
20. Saenz DT, Fiskus W, Qian Y, et al. Novel BET protein proteolysis-targeting chimera exerts superior lethal activity than bromodomain inhibitor (BETi) against post-myeloproliferative neoplasm secondary (s) AML cells. *Leukemia*. 2017;31(9):1951-1961.
21. Itoh Y, Kitaguchi R, Ishikawa M, Naito M, Hashimoto Y. Design, synthesis and biological evaluation of nuclear receptor-degradation inducers. *Bioorg Med Chem*. 2011;19(22):6768-6778.
22. Demizu Y, Okuhira K, Motoi H, et al. Design and synthesis of estrogen receptor degradation inducer based on a protein knockdown strategy. *Bioorg Med Chem Lett*. 2012;22(4):1793-1796.
23. Lai AC, Toure M, Hellerschmied D, et al. Modular PROTAC design for the degradation of oncogenic BCR-ABL. *Angew Chem Int Ed Engl*. 2016;55(2):807-810.
24. Gao S, Wang S, Song Y. Novel immunomodulatory drugs and neo-substrates. *Biomark Res*. 2020;8:2.
25. Pettersson M, Crews CM. Proteolysis targeting chimeras (PROTACs) - past, present and future. *Drug Discov Today Technol*. 2019;31:15-27.
26. Sun X, Gao H, Yang Y, et al. PROTACs: great opportunities for academia and industry. *Signal Transduct Target Ther*. 2019;4:64.
27. Leiser D, Pochon B, Blank-Liss W, et al. Targeting of the MET receptor tyrosine kinase by small molecule inhibitors leads to MET accumulation by impairing the receptor downregulation. *FEBS Lett*. 2014;588(5):653-658.
28. Reiff SD, Mantel R, Smith LL, et al. The BTK inhibitor ARQ 531 targets ibrutinib-resistant CLL and Richter transformation. *Cancer Discov*. 2018;8(10):1300-1315.
29. Buhimschi AD, Armstrong HA, Toure M, et al. Targeting the C481S Ibrutinib-resistance mutation in Bruton's tyrosine kinase using PROTAC-mediated degradation. *Biochemistry*. 2018;57(26):3564-3575.
30. Burslem GM, Smith BE, Lai AC, et al. The advantages of targeted protein degradation over inhibition: an RTK case study. *Cell Chem Biol*. 2018;25(1):67-77.e63.
31. Paul J, Soujon M, Wengner AM, et al. Simultaneous inhibition of PI3Kδ and PI3Kα induces ABC-DLBCL regression by blocking BCR-dependent and -independent activation of NF-κB and AKT. *Cancer Cell*. 2017;31(1):64-78.
32. Takahashi K, Sivina M, Hoellenriegel J, et al. CCL3 and CCL4 are biomarkers for B cell receptor pathway activation and prognostic serum markers in diffuse large B cell lymphoma. *Br J Haematol*. 2015;171(5):726-735.
33. Sun Y, Ding N, Song Y, et al. Degradation of Bruton's tyrosine kinase mutants by PROTACs for potential treatment of ibrutinib-resistant non-Hodgkin lymphomas. *Leukemia*. 2019;33(8):2105-2110.
34. Asatsuma-Okumura T, Ito T, Handa H. Molecular mechanisms of cereblon-based drugs. *Pharmacol Ther*. 2019;202:132-139.

35. Chamberlain PP, Cathers BE. Cereblon modulators: low molecular weight inducers of protein degradation. *Drug Discov Today Technol*. 2019;31:29-34.

36. Lu G, Middleton RE, Sun H, et al. The myeloma drug lenalidomide promotes the cereblon-dependent destruction of Ikaros proteins. *Science*. 2014;343(6168):305-309.

37. Burger JA. Inhibiting B-cell receptor signaling pathways in chronic lymphocytic leukemia. *Curr Hematol Malig Rep*. 2012;7(1):26-33.

38. George B, Chowdhury SM, Hart A, et al. Ibrutinib resistance mechanisms and treatment strategies for B-cell lymphomas. *Cancers*. 2020;12(5).

39. de Claro RA, McGinn KM, Verdun N, et al. FDA approval: ibrutinib for patients with previously treated mantle cell lymphoma and previously treated chronic lymphocytic leukemia. *Clin Cancer Res*. 2015;21(16):3586-3590.

40. Gángó A, Alpár D, Galik B, et al. Dissection of subclonal evolution by temporal mutation profiling in chronic lymphocytic leukemia patients treated with ibrutinib. *Int J Cancer*. 2020;146(1):85-93.

41. Li T, Tsukada S, Satterthwaite A, et al. Activation of Bruton's tyrosine kinase (BTK) by a point mutation in its pleckstrin homology (PH) domain. *Immunity*. 1995;2(5):451-460.

42. Wang Q, Pechersky Y, Sagawa S, Pan AC, Shaw DE. Structural mechanism for Bruton's tyrosine kinase activation at the cell membrane. *Proc Natl Acad Sci U S A*. 2019;116(19):9390-9399.

43. Sharma S, Galanina N, Guo A, et al. Identification of a structurally novel BTK mutation that drives ibrutinib resistance in CLL. *Oncotarget*. 2016;7(42):68833-68841.

44. Li X, Song Y. Proteolysis-targeting chimera (PROTAC) for targeted protein degradation and cancer therapy. *J Hematol Oncol*. 2020;13(1):50.

45. Lai AC, Crews CM. Induced protein degradation: an emerging drug discovery paradigm. *Nat Rev Drug Discov*. 2017;16(2):101-114.

46. Raina K, Lu J, Qian Y, et al. PROTAC-induced BET protein degradation as a therapy for castration-resistant prostate cancer. *Proc Natl Acad Sci U S A*. 2016;113(26):7124-7129.

47. Nguyen TM, Deb A, Kokkonda P, et al. Proteolysis targeting chimeras with reduced off-targets. *bioRxiv*. 2021, 2021:2011.2018.468552.

48. Wang H, Hu H, Zhang Q, et al. Dynamic transcriptomes of human myeloid leukemia cells. *Genomics*. 2013;102(4):250-256.

49. Trojani A, Di Camillo B, Bossi LE, et al. Identification of a candidate gene set signature for the risk of progression in IgM MGUS to smoldering/symptomatic Waldenström macroglobulinemia (WM) by a comparative transcriptome analysis of B cells and plasma cells. *Cancers*. 2021;13(8).